Hybrid plasmonic waveguides for low-threshold nanolaser applications

Hongbo Lv (吕宏博)[1*], Yumin Liu (刘玉敏)[1,2], Zhongyuan Yu (俞重远)[1], Chunwei Ye (叶春伟)[1], and Jie Wang (汪 洁)[1]

[1]*State Key Laboratory of Information Photonics and Optical Communications, Beijing University of Posts and Telecommunications, Beijing 100876, China*

[2]*State Key Laboratory of Integrated Optoelectronics, Institute of Semiconductors, Chinese Academy of Sciences, Beijing 100083, China*

[*]*Corresponding author: 705456415@qq.com*

Received June 20, 2014; accepted August 8, 2014; posted online October 15, 2014

We propose new types of hybrid plasmonic waveguides for low-threshold nanolaser applications. Modal properties and lasing threshold under different geometric shapes and parameters are investigated and analyzed by the finite element method, aiming to realize both low propagation and high field confinement. Results show that a smaller gap width and a larger round corner radius of the metal film reduce the lasing threshold. These new structures can open up new avenues in the fields of active plasmonic circuits.

OCIS codes: 240.6680, 140.5960, 350.5500.

doi: 10.3788/COL201412.112401.

Since the first laser was produced 50 years ago, laser science has attracted more and more attention and has been successful in producing increasingly high-powered, faster, and more compact coherent light sources[1]. Research into microscopic lasers based on photonic crystals metal-clad cavities and nanowires has also achieved great advances recently. However, the size of a dielectric optical cavity of such lasers must be larger than the half wavelength of the optical field in all three dimensions due to the diffraction limitation[2]. In order to remove this limitation, surface plasmons can be used. This method has achieved great progress in overcoming the limitation in optics. A team has demonstrated a viable material platform for the construction of integrated dielectric–plasmon circuits by using silicon-on-insulator (SOI) wafers that are commercially available[3–13].

Surface plasmons, free electron density waves propagating along the dielectric–metal interface, are produced by the interaction of the electrons and photons. They can allow the compact storage of optical energy in electron oscillations at the interfaces and offer the best confinement for the light field. This property is used to create subwavelength waveguides and cavities[6, 14–22]. The main challenge associated with plasmonic cavities is the loss that mainly comes from metal absorption. Realizing both low propagation and high field confinement is very important.

In this letter, we propose and compare some modals by maintaining modes in a hybrid plasmonic waveguide to reduce the loss and analyze the lasing threshold under different geometric shapes and parameters of models. Here we use the COMSOL software to investigate the properties by the finite element method. Scattering boundary condition and convergence tests are used to ensure the solution accuracy.

The first proposed structure is shown in Fig. 1(a). It consists of two pieces of semi-infinite thin silver film with sharp corners on the sides of the high-index nanowire for symmetry deposited on the MgF_2 substrate. The gain material used for the nanowire with radius r is CdS. The thickness of the silver film is $2r$ and the minimal width of the gap between the silver film and the CdS nanowire is h. In the simulation, the permittivity of the CdS, MgF_2, and silver are 1.96, 5.76 and $-9.2+0.3i$, respectively. The high-index CdS nanowire, low-index air gap, and MgF_2 substrate support hybrid plasmonic modes with low propagation loss and high field confinement. The close proximity of the nanowire and metal interfaces concentrates light into an extremely small area as much as a hundred times smaller than a diffraction-limited spot[23]. The wavelength is fixed at 490 nm and the parameters are chosen to be consistent with Ref. [24].

From the electric field distribution, shown in Fig. 1(b), we can find that most of the energy is concentrated within the gap between the thin silver films. There are two reasons accounting for this. First, it arises from the continuity of the displacement field at the material interfaces, which leads to a strong normal

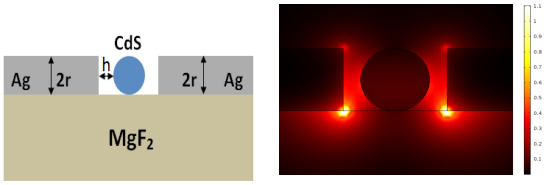

(a) (b)

Fig. 1(a) Geometry of edge-coupled hybrid plasmonic waveguide with bilateral silver films. (b) Electric field distribution of the fundamental mode ($r = 60$ nm).

electric field component in the gap. Second, in both uncoupled surface plasmon polariton (SPP) and cylinder geometries, the electric field components normal to the material interfaces are dominant, amplifying the first effect.

The mode property and lasing threshold of the modal are important indexes to characterize the feature of nanolaser. The modal effective index n_{eff}, effective propagation loss α_{eff}, normalized mode area A_{eff}/A_0, and confinement factor Γ can reflect the mode property. n_{eff} and α_{eff} are the real part of the hybrid waveguide propagation constant and the imaginary part over the free-space wave vector, respectively. The effective mode area A_{eff} is defined as

$$A_{\text{eff}} = \frac{\left(\int\int |E|^2 \, \mathrm{d}x\mathrm{d}y\right)^2}{\left(\int\int |E|^4 \, \mathrm{d}x\mathrm{d}y\right)}. \tag{1}$$

The diffraction-limited mode area is calculated by using $A_0 = \lambda^2/4$. The confinement factor Γ is defined as the ratio of the electric energy in the CdS nanowire to the total electric energy of the mode. The electric energy density distributions $W(x,y)$ is calculated by

$$W(x,y) = \frac{1}{2}\mathrm{Re}\left[\frac{\mathrm{d}(\varepsilon(x,y)\omega)}{\mathrm{d}\omega}\right]\left|E(x,y)\right|^2, \tag{2}$$

where $\left|E\left(x,y\right)\right|^2$ is the intensity of the electric field. The lasing threshold is calculated by using the formula

$$g_{\text{th}} = (k_0\ \alpha_{\text{eff}} + \ln(1/R)/L)\Gamma\ (n_{\text{eff}}/n_{\text{wire}}). \tag{3}$$

Here the reflectivity is calculated by using $R = (n_{\text{eff}} - 1)/(n_{\text{eff}} + 1)$, n_{wire} is the refractive index of the nanowire and the nanowire length L is set to be 30 μm.

Figure 2 shows that the increase in the gap width leads to the increase in the normalized area and the decrease in mode effective index, effective propagation loss, and confinement factor. The normalized mode area is below 0.2, indicating the deep-subwavelength mode confinement. Our results also indicate that the threshold increases when the width of the gap grows from 2.5 to 30 nm. When the width of the gap remains the same, the threshold decreases as the radius of the nanowire increases.

To investigate whether the corner radius affects the modal properties, the sharpness of the metal film corners is reduced. The top and bottom corners of the metal edge of the first structure are designed to have the same radius r_c, and the gap width is set to be 5 nm, as shown in Fig. 3.

Figure 4 shows that the increase in the radius r_c leads to the increase in the confinement factor and the decrease in mode effective index, effective propagation loss, and normalized area. From Fig. 4(a), we can find that when r_c is smaller than 35 nm, smaller radius of the nanowire results in larger n_{eff}, while the trend is opposite after that. The threshold reduces obviously

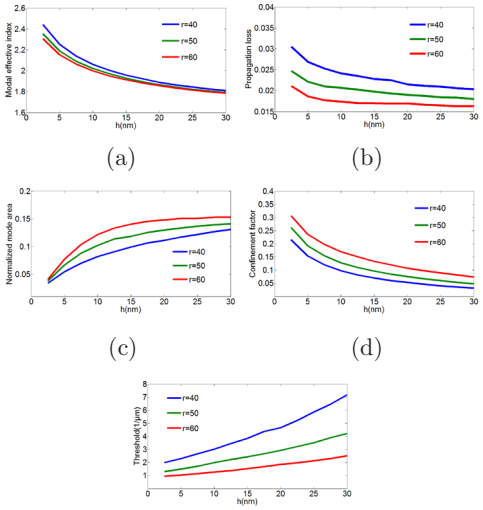

Fig. 2(a) Modal effective index. (b) Effective propagation loss. (c) Normalized mode area. (d) Confinement factor of the fundamental mode at different air gap widths with different radii of nanowire. (e) Dependence of lasing threshold on air gap widths.

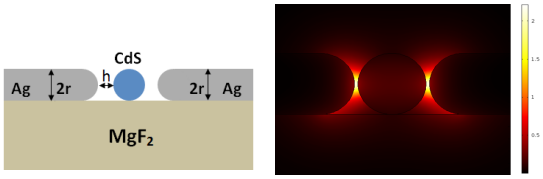

Fig. 3(a) Geometry of edge-coupled hybrid plasmonic waveguide with bilateral silver films and the radius of metal edge corners is r_c. (b) Electric field distribution of the fundamental mode ($r = 50$ nm)..

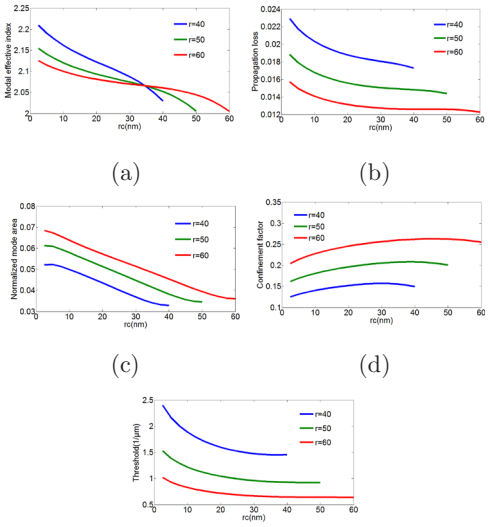

Fig. 4(a) Modal effective index. (b) Effective propagation loss. (c) Normalized mode area. (d) Confinement factor of the fundamental mode with different radii of the bilateral silver film corners. (e) Dependence of lasing threshold on the corner radius.

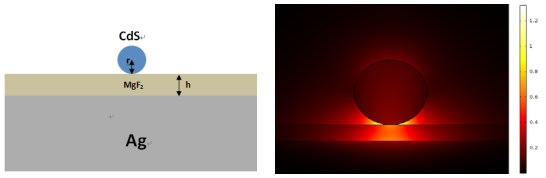

(a) (b)

Fig. 5(a) Geometry of the plasmonic waveguide. (b) Electric field distribution of the fundamental mode.

as radius r_c increases until the threshold levels are off when r_c approaches the radius of the nanowire r. So increasing the corner radius is helpful for reducing the threshold.

Comparing with some other edge-coupled hybrid waveguide structures, which consist of one piece of semi-infinite thin silver film with sharp or round corners on the side of the nanowire on the MgF_2 substrate, we have reduced the lasing threshold respectively.

The next structure of the plasmonic waveguide consists of a CdS nanowire on top of a silver substrate, separated by a MgF_2 layer. The radius of the nanowire is r and the thickness of the layer is h, as shown in Fig. 5.

From the electric field distribution of the fundamental mode, we can see that most of the energy is concentrated between the nanowire and the MgF_2 substrate. In this way, surface plasmon polaritons can travel longer with strong mode confinement.

Figure 6 shows that the threshold decreases rapidly with the increase in small gap width at first and increases slowly when the width becomes larger. The threshold is below $1/(\mu m)$ when the width grows from 2.5 to 30 nm.

Comparing with the research on hybrid plasmon waveguide in Ref. [24], we have theoretically analyzed the mode property and lasing threshold of the model to reduce the threshold and proposed new designs at the base of this. In this structure, a nanowire waveguide with the radius r is placed on a substrate. The material between the nanowire and metal is air and the gap's width is h, as shown in Fig. 7.

Figure 8 indicates that the threshold increases when the width of the gap grows from 2.5 to 30 nm and when the width of the gap is same, the threshold decreases with larger radius of the nanowire.

In order to investigate the effect of the sharpness of the metal film corners on the characteristics of this structure, the left and right corners of the metal edge near the nanowire are assumed to have the same radius r_c, as shown in Fig. 9.

Figure 10 shows that the lasing threshold reduces more and more slowly as radius r_c increases with larger radius of the nanowire leading to smaller thresholds.

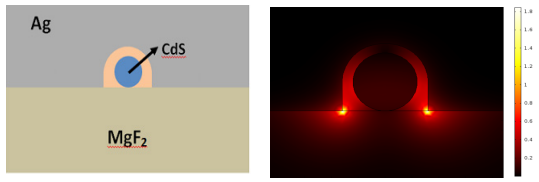

(a) (b)

Fig. 7(a) Geometry of the plasmonic waveguide with air gap. (b) Electric field distribution of the fundamental mode ($h = 30$ nm).

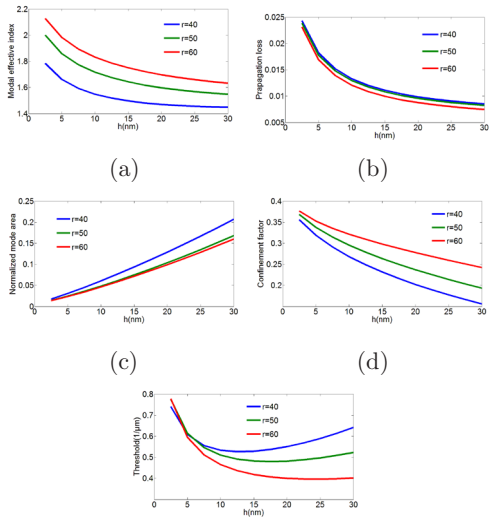

(a) (b) (c) (d) (e)

Fig. 6(a) Modal effective index. (b) Effective propagation loss. (c) Normalized mode area. (d) Confinement factor of the fundamental mode at different MgF_2 gap widths with different radii of nanowire. (e) Dependence of lasing threshold on MgF_2 gap widths.

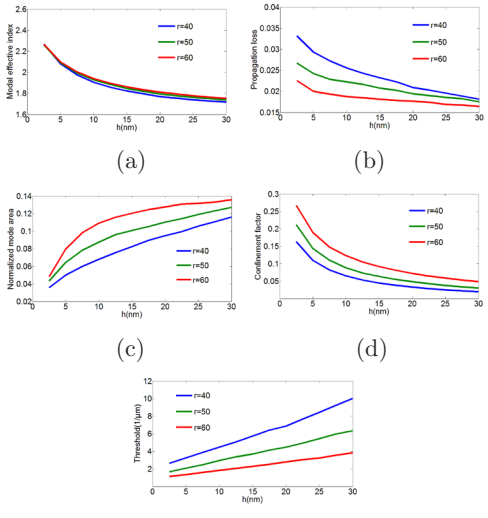

(a) (b) (c) (d) (e)

Fig. 8(a) Modal effective index. (b) Effective propagation loss. (c) Normalized mode area. (d) Confinement factor of the fundamental mode at different gap widths with different radii of nanowire. (e) Dependence of lasing threshold on gap widths.

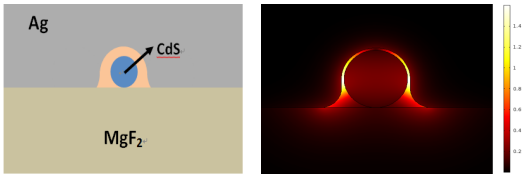

(a) (b)

Fig. 9(a) Geometry of the plasmonic waveguide with air gap and the radius of the metal edge corners is r_c. (b) Electric field distribution of the fundamental mode (r_c = 5 nm).

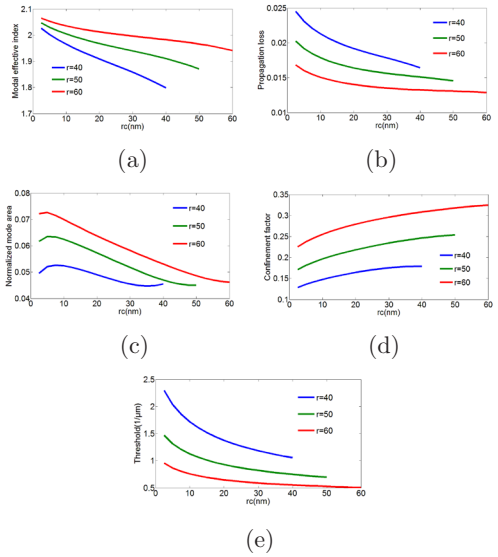

(a) (b) (c) (d) (e)

Fig. 10(a) Modal effective index. (b) Effective propagation loss. (c) Normalized mode area. (d) Confinement factor of the fundamental mode with different radii of the silver film corners. (e) Dependence of lasing threshold on corner radius of the metal film.

Therefore smaller gap width and the metal film with relatively larger corner radius of the metal film will be helpful for the reduction of the threshold in these structures.

In conclusion, we propose novel types of hybrid plasmonic waveguides for low-threshold nanolaser applications. We analyze the effect of the geometric shape and parameters on modal properties and lasing threshold. We find that the theoretical threshold can be reduced by decreasing both the gap width and the corner radius of the metal films. The structures can be realized using a relatively simple fabrication process and are useful for further active plasmonic circuits.

This work was supported by the National Natural Science Foundation of China (Nos. 61275201 and 61372037), the Beijing Excellent Ph.D. Thesis Guidance Foundation (No. 20131001301), the Fund of State Key Laboratory of Information Photonics and Optical Communications (Beijing University of Posts and Telecommunications), and the Open Fund of the State Key Laboratory on Integrated Optoelectronics, Institute of Semiconductors, Chinese Academy of Sciences.

References

1. X. F. Duan, Y. Huang, R. Agarwal, and C. M. Lieber, Nature **421,** 241 (2003).
2. L. Zhu, IEEE Photon. Technol. Lett. **22,** 535 (2010).
3. Y. Shen, G. Yu, J. Fu, and L. Zou, Chin. Opt. Lett. **10,** 021301 (2012).
4. K. Wen, L. Yan, W. Pan, Z. Guo, and Y. Guo, Chin. Opt. Lett. **10,** S22301 (2012).
5. Y. Wang, Y. Ma, X. Guo, and L. Tong, Opt. Express **20,** 19006 (2012).
6. E. Ozbay, Science **311,** 189 (2006).
7. X. Guo, M. Qiu, J. M. Bao, B. J. Wiley, Q. Yang, X. N. Zhang, Y. G. Ma, H. K. Yu, and L. M. Tong, Nano Lett. **9,** 4515 (2009).
8. R. M. Dickson and L. A. Lyon, J. Phys. Chem. B **104,** 6095 (2000).
9. S. A. Maier, P. G. Kik, H. A. Atwater, S. Meltzer, E. Harel, B. E. Koel, and A. A. Requicha, Nat. Mater **2,** 229 (2003).
10. J. Jung, T. Sondergaard, and S. I. Bozhevolnyi, Phys. Rev. B **76,** 035434 (2007).
11. U. Schroter and A. Dereux, Phys. Rev. B **64,** 125420 (2001).
12. G. Veronics and S. Fan, J. Lightw. Technol. **25,** 2511 (2007).
13. M. Hochberg, T. Baehr-Jones, C. Walker, and A. Scherer, Opt. Express **12,** 5481 (2004).
14. A. M. Lerer, I. V. Donets, G. A. Kalinchenko, and P. V. Makhno, Photon. Res. **2,** 31 (2014).
15. R. D. Roy, R. Chattopadhyay, and S. K. Bhadra, Photon. Res. **1,** 164 (2013).
16. C. C. Huang, IEEE J. Sel. Top. Quant. Electron. **18,** 1661 (2012).
17. Y. Bian, Z. Zheng, X. Zhao, J. Zhu, and T. Zhou, Opt. Express **17,** 21320 (2009).
18. R. F. Oulton, V. J. Sorger, D. A. Genov, D. F. P. Pile, and X. Zhang, Nat. Photon. **2,** 496 (2008).
19. W. L. Barnes, A. Dereux, and T. W. Ebbesen, Nature **424,** 824 (2003).
20. S. A. Maier and H. A. Atwater, J. Appl. Phys. **98,** 011101 (2005).
21. M. L. Brongersma, *Surface Plasmon Nanophotonics* (Springer, New York, 2007).
22. V. M. Shalaev and S. Kawata, *Nanophotonics with Surface Plasmons* (Elsevier, Amsterdam, 2007).
23. A. Maslov and C. Z. Ning, Proc. SPIE **6468,** 646801 (2007).
24. Y. Yin, T. Qiu, J. Li, and P. K. Chu, Nano Energy **1,** 25 (2012).